A Plasma Metabolomic Signature of the Exfoliation Syndrome Involves Amino Acids, Acylcarnitines, and Polyamines

Stéphanie Leruez,[1,2] Thomas Bresson,[2] Juan M. Chao de la Barca,[1,3] Alexandre Marill,[2] Grégoire de Saint Martin,[2] Adrien Buisset,[2] Jeanne Muller,[2,4] Lydie Tessier,[3] Cédric Gadras,[3] Christophe Verny,[4] Patrizia Amati-Bonneau,[1,3] Guy Lenaers,[1] Philippe Gohier,[2] Dominique Bonneau,[1,3] Gilles Simard,[3,5] Dan Milea,[6] Vincent Procaccio,[1,3] and Pascal Reynier[1,3]

[1]Equipe Mitolab, Institut MITOVASC, UMR CNRS 6015, INSERM U1083, Université d'Angers, Angers, France
[2]Département d'Ophtalmologie, Centre Hospitalier Universitaire, Angers, France
[3]Département de Biochimie et Génétique, Centre Hospitalier Universitaire, Angers, France
[4]Département de Neurologie, Centre Hospitalier Universitaire, Angers, France
[5]INSERM U1063, Université d'Angers, Angers, France
[6]Singapore Eye Research Institute, Singapore National Eye Centre, Duke-NUS, Singapore

Correspondence: Stéphanie Leruez, Département d'Ophtalmologie, Centre Hospitalier Universitaire, 4 rue Larrey, F-49933 Angers, France; stleruez@chu-angers.fr.

Submitted: September 26, 2017
Accepted: January 8, 2018

Citation: Leruez S, Bresson T, Chao de la Barca JM, et al. A plasma metabolomic signature of the exfoliation syndrome involves amino acids, acylcarnitines, and polyamines. *Invest Ophthalmol Vis Sci*. 2018;59:1025–1032. https://doi.org/10.1167/iovs.17-23055

Purpose. To determine the plasma metabolomic signature of the exfoliative syndrome (XFS), the most common cause worldwide of secondary open-angle glaucoma.

Methods. We performed a targeted metabolomic study, using the standardized p180 Biocrates Absolute IDQ p180 kit with a QTRAP 5500 mass spectrometer, to compare the metabolomic profiles of plasma from individuals with XFS ($n = 16$), and an age- and sex-matched control group with cataract ($n = 18$).

Results. A total of 151 metabolites were detected correctly, 16 of which allowed for construction of an OPLS-DA model with a good predictive capability (Q^2cum = 0.51) associated with a low risk of over-fitting (permQ2 = −0.48, CV-ANOVA *P*-value <0.001). The metabolites contributing the most to the signature were octanoyl-carnitine (C8) and decanoyl-carnitine (C10), the branched-chain amino acids (i.e., isoleucine, leucine, and valine), and tyrosine, all of which were at higher concentrations in the XFS group, whereas spermine and spermidine, together with their precursor acetyl-ornithine, were at lower concentrations than in the control group.

Conclusions. We identified a significant metabolomic signature in the plasma of individuals with XFS. Paradoxically, this signature, characterized by lower concentrations of the neuroprotective spermine and spermidine polyamines than in controls, partially overlaps the plasma metabolomic profile associated with insulin resistance, despite the absence of evidence of insulin resistance in XFS.

Keywords: exfoliation syndrome, exfoliative glaucoma, metabolomics, glaucoma

Initially described by Lindberg,[1] the exfoliative syndrome (XFS) is defined as an age-related systemic fibrillopathy due to excessive production and progressive accumulation of fibrillar deposit in the extracellular matrix of organs. The eyes, where the fibrillar deposit accumulates in the anterior segment and outflow pathways, are one of the main targets of the disease. XFS, is the most common cause of secondary open-angle glaucoma or exfoliative glaucoma (XFG), which may account for 5 to 6 million cases of the disease among the 70 million people affected by XFS worldwide, and for approximately 10% of patients with glaucoma.[2]

Blockage of aqueous outflow by exfoliation material deposited in the intertrabecular spaces, in the juxtacanalicular meshwork, and under the endothelium of Schlemm's canal is believed to be the major cause of elevated IOP.[2] XFG is characterized mainly by bilateral and asymmetric eye damage, with glaucoma usually more severe than in the case of primary open-angle glaucoma. The rate of visual field degradation and optic nerve damage at diagnosis is faster in XFG than in primary open-angle glaucoma, with a poorer response to treatment, quicker progression, greater recourse to surgery, and a larger proportion of blindness.[3,4] The other ocular damages related to XFS are cataract, zonular laxity, iritic vascular damage, and corneal endothelial damage. The main extraocular complications are cardiovascular and cerebrovascular involvements, including stroke, myocardial infarction, hypertension, aortic aneurysm, and peripheral vascular disease, together with the risk of hearing loss, cerebral atrophy, and Alzheimer's disease.[2,5]

XFS is a complex, multifactorial disorder related to the ageing process as well as genetic and environmental factors. Considerable progress has been made in the search for disease biomarkers by high-throughput "omics" investigations. Common variants in the *LOXL1* (lysine-oxydase-like 1) and

CACNA1A (α1A subunit of the type P/Q voltage-dependent calcium channel) genes were shown to increase susceptibility to XFS and XFG.[6,7] More recently, a protective *LOXL1* variant and five new susceptibility loci have been reported to be involved in protecting against XFS.[8] Transcriptomic investigations in the aqueous humor, serum, and tissues have shown that XFS is related to the excessive production of elastic microfibril components, overexpression of the TGF-β1 and increased oxidative stress, together with an impaired cellular stress response.[2] In addition, proteomics studies have shown a large number of proteins within the ocular exfoliative material, such as LOXL1, apolipoprotein E (ApoE), latent–TGF-β–binding protein-2 (LTBP-2), complement 3, clusterin proteins, fibrillin-1, fibronectin, vitronectin, laminin, amyloid P component, tissue inhibitor of metalloproteinase 3 (TIMP-3), fibulin-2, desmocollin-2, and the glycosaminoglycan syndecan-3.[9] Currently, the main pathomechanisms of XFS and the consequent dysfunctions are considered to involve growth factors and cytokines, alteration of TGF-β1, matrix metalloproteinases (MMPs) and their endogenous tissue inhibitors of metalloproteinases (TIMPs), hyper-homocysteinemia and alteration of the folate metabolism, increased oxidative stress response, impaired autophagy and mitochondrial function, and hypoxia related to vasculopathy.[5]

Further downstream in the "omics" cascade, although metabolomics holds good promise for the discovery of new biomarkers, to our knowledge, it has never been applied to the blood of individuals with XFS or XFG. We used a standardized targeted metabolomics approach to search for biomarkers in the plasma of XFS patients compared to sex- and age-matched controls with cataract.

Materials and Methods

Ethics Statement

The study was conducted in accordance with the ethical standards set forth in the Declaration of Helsinki (1983) and was approved by the University of Angers Ethical Review Committee (CPP OUEST 2, agreement number: CB 2013-04). Participants were included after having given their informed written consent for research.

Study Participants

Individuals were recruited from the Department of Ophthalmology at the Angers University Hospital, France. All individuals with XFS and controls underwent an extensive ophthalmic examination, including slit-lamp evaluation after dilatation of the pupil, optic disc biomicroscopy, assessment of the central corneal thickness (CCT), and retinal nerve fiber layer (RNFL) with spectral domain optical coherence tomography (OCT; Cirrus OCT; Carl Zeiss Meditec, Dublin, CA, USA). The best-corrected visual acuity was measured using the Monoyer decimal optometric charts, with the results converted into logMAR units for statistical analysis. IOP was measured using Goldmann applanation tonometry. Treatment and medical histories of all XFS patients, including eventual comorbidities, were documented electronically.

XFS was diagnosed based on a complete or partial peripheral band and/or a central shield of exfoliative material on the anterior lens capsule of at least one eye.[3] Gonioscopic examination showed open iridocorneal angles in all cases. Patients with open-angle glaucomatous optic nerve damage and optic nerve cupping were diagnosed as having XFG. Standard automated perimetry (Humphrey Field Analyzer; Carl Zeiss Meditec) using the 24-2 SITA-fast algorithm was performed for patients with XFG. The values of the visual field mean defect (VF-MD) were used to grade the severity of the disease as "mild" (values lower than –6 dB), "moderate" (values between –6 and –12 dB), and "severe" (values higher than –12 dB; perimetric Hoddap-Parrish-Anderson criteria).[10] The reliability indices retained were false-positive or false-negative rates under 15%, and fixation losses under 20%. No repetition of the standard automated perimetry was performed.

Control subjects were selected among individuals undergoing cataract surgery at the same department of ophthalmology, the inclusion criteria being visual acuity ≥20/50 with no other ocular pathology except cataract. Exclusion criteria were based on personal reasons or because of a family history of XFS, ocular hypertension, glaucoma, or other intraocular pathologies, including retinal disorders. The control group ($n = 20$) was age- and sex-matched to the XFS/XFG group of patients ($n = 20$).

Sample Collection

Fasting blood samples were collected in heparin tubes at the department of ophthalmology, transported rapidly in crushed ice to the Hospital Biological Resources Center, and centrifuged immediately for 10 minutes at 3000*g* at +4°C before recovery of the supernatant (plasma), which was conserved at –80°C in 500 µL aliquots until metabolomics analysis.

Metabolomics Analysis

Targeted quantitative metabolomics analysis was performed using the Biocrates Absolute IDQ p180 kit (Biocrates Life Sciences AG, Innsbruck, Austria). This kit uses mass spectrometry (QTRAP 5500; SCIEX, Villebon-sur-Yvette, France) to quantify up to 188 different endogenous molecules distributed as follows: free carnitine (C0), 39 acylcarnitines (C), the sum of hexoses (H1), 21 amino acids, 21 biogenic amines, and 105 lipids. Lipids are distributed in the kit in four different classes: 14 lysophosphatidylcholines (lysoPC), 38 diacyl-phosphatidylcholines (PC aa), 38 acyl-alkyl-phosphatidylcholines (PC ae), and 15 sphingomyelins (SM). The full list of individual metabolites is available in the public domain at http://www.biocrates.com/products/research-products/absoluteidq-p180-kit. Flow injection analysis coupled with tandem mass spectrometry (FIA-MS/MS) was used for analysis of carnitine, acylcarnitines, lipids, and hexoses. Liquid chromatography (LC) was used for separating amino acids and biogenic amines before quantitation with mass spectrometry.

All reagents used in this analysis were of LC-MS grade and purchased from VWR (Fontenay-sous-Bois, France) and Merck (Molsheim, France). Sample preparation and analyses were performed following the Kit User Manual. Briefly, each plasma sample was vortexed thoroughly after thawing and centrifuged at 4°C for 5 minutes at 5000*g*. Ten microliters of each sample were mixed with isotopically labeled internal standard in a multititer plate and dried under nitrogen flow (nitrogen evaporator 96 well plate; Stuart SBM 200 D/3, Stuart, Stone, UK). Metabolites then were derivatized with phenylisothiocyanate (PITC) 5% for 20 minutes at room temperature and subsequently dried for 30 minutes under nitrogen flow. For extraction, first 300 µL extraction solvent (5 mM ammonium acetate in methanol) were added and incubated with shaking at 450 revolutions per minute (IKA MS3 digital, Thermo Fisher Scientific, Illkrich, France) for 30 minutes at room temperature, followed by filtration by centrifugation (Hettich Zentrifugen Rotina 380R, Bäch, Switzerland) for 2 minutes at 500*g*. Subsequently, 200 µL were removed from the filtrate, transferred to a fresh multititer deep-well plate, and diluted

with 200 μL water for LC–MS analysis of biogenic amines and amino acids. To the remaining 100 μL from the filtrate, 500 μL MS running solvent were added for FIA-MS/MS. Both types of measurement were performed on a QTRAP mass spectrometer applying electrospray ionization (ESI; AB Sciex API5500Q-TRAP, SCIEX, Villebon-sur-Yvette, France). The MS was coupled to a high-performance liquid chromatograph (HPLC; Agilent Technologies 1200 series, Les Ulis, France). In the case of LC–MS, the metabolites were separated by a hyphenated reverse phase column (Agilent, Zorbax Eclipse XDB C18, 3.0 × 100 mm, 3.5 μm) preceded by a pre-column (Security Guard, Phenomenex, C18, 4 × 3 mm. Phenomenex, Torrance, CA, USA) applying a gradient of solvent A (formic acid 0.2% in water) and solvent B (formic acid 0.2% in acetonitrile) over 7.3 minutes (0.5 minutes 0% B, 5 minutes 70% B, 0.3 minutes 70% B, 2 minutes 0% B) at a flow rate of 500 μL/min. The oven temperature was 50°C. For LC-MS analysis and for FIA, 10 and 2 × 20 μL samples, respectively, were subjected to measurements in the positive and negative modes. The identification and quantification were achieved by multiple reactions monitoring (MRM) standardized by applying spiked-in isotopically labelled standards in the positive and negative modes, respectively. For calibration, a calibrator mix consisting of seven different concentrations was used. Quality controls derived from lyophilized human plasma samples were included for 3 different concentration levels. For FIA, an isocratic method was used (100% organic running solvent) with varying flow conditions (0 minutes, 30 μL/min; 1.6 minutes 30 μL/min; 2.4 minutes, 200 μL/min; 2.8 minutes, 200 μL/min; 3 minutes 30 μL/min). The MS settings were as follows: scan time 0.5 seconds; IS voltage for positive mode 5500 V, for negative mode –4500 V; source temperature 200°C; with nitrogen as the collision gas medium. The corresponding parameters for LC–MS were: scan time 0.5 seconds, source temperature 500°C, with nitrogen as the collision gas medium. All reagents used in the processing and analysis were of LC–MS grade, unless otherwise stated. Milli-Q Water ultrapure was used fresh after being prepared by the high-purity water system with Millipore (Milli-Di). The raw data of the Analyst software (AB Sciex, Framingham, MA, USA) were processed by the MetIDQ software, which is an integral part of the p180 Kit (Biocrates Life Sciences AG). This streamlines data analysis by the automated calculation of metabolite concentrations providing quality measurements and quantification. For fully quantitative measurements of the p180 Kit, the lower limit of quantification (LLOQ) was determined experimentally in plasma by Biocrates Life Sciences AG.

Statistical Analysis

Before statistical analysis, the raw data were examined to exclude metabolites with more than 20% of concentration values below the LLOQ or above the upper limit of quantitation (ULOQ).

Multivariate analysis was performed first using principal component analysis (PCA) for the detection of sample grouping and outliers. Orthogonal partial least squares discriminant analysis (OPLS-DA) then was applied to maximize variation between the XFS and control groups, and to determine the metabolites contributing to this variation. Multivariate analyses for the PCA and OPLS-DA models were performed on mean-centered and unit variance-scaled (MC-UV) data. The quality of the OPLS-DA model was validated by two parameters; that is, goodness of fit (R^2) and goodness of prediction indicated by the cumulated Q^2 value (Q^2cum). A threshold of 0.5 was used to determine whether an OPLS-DA model could be estimated as having a good ($Q^2\text{cum} \geq 0.5$) or poor ($Q^2\text{cum} < 0.5$) predictive capability.[11] To avoid overfitting, variables considered superfluous based on the variable importance for the projection (VIP) and the loading values were eliminated from the initial model using a backward procedure. VIP values summarized the importance of each variable for the OPLS-DA model, whereas the loading values were indicators of the relationship between the y vector containing the class information (i.e., XFS or Control) and variables in the X matrix (i.e., metabolites). Variables with a VIP value greater than unity are important for group discrimination in predictive models.[11] The risk of overfitting and the robustness of the final reduced model were assessed by the intercept of the permutation plot ($permQ_2$) and cross-validated analysis of variance (CV-ANOVA). Nonoverfitted models have a negative permQ2 intercept and are considered significantly different from models obtained randomly with the CV-ANOVA test at $P < 0.05$. In the reduced model, plotting key variables based on VIP values versus loading values scaled as correlation coefficients (p_{corr}) yields a V-shaped graph known as the "volcano" plot, on which the most important variables are easily recognized. Multivariate data analysis was conducted using SIMCA-P v.14.0 (Umetrics, Umeå, Sweden).

Univariate analysis was performed using the bilateral Student's *t*-test and differences were considered significant at $P \leq 0.05$.

Table 1. Demographic Data and Comorbidity Status of XFS/XPG Patients Compared to Controls

	XFS/XFG, $N = 18$	Controls, $N = 16$	P Values
Average age, y	75.55	74.12	0.45
Females, %	44.44	37.5	0.69
Mean BMI, kg/m^2	25.33	26.24	0.47
Diabetes, %	22.22	12.5	0.38
Hypertension, %	44.44	56.25	0.51
Hyperlipidemia, %	33.33	50	0.36
Thyroid disease, %	0	12.5	0.16

Results

Clinical Features of XFS/XFG Patients and Controls

Six blood samples obtained from the 20 individuals with XFS/XFG and 20 controls initially included in the study had to be rejected because of hemolysis, leaving 18 XFS/XFG and 16 control individuals. Table 1 presents the demographic and environmental data, as well as comorbid medical conditions, of these patients and controls. Mean age of individuals with XFS/XFG did not differ significantly from that of controls, nor did the sex ratio. There was no between-group difference regarding hypertension, hyperlipidemia, diabetes, body mass index (BMI), or thyroid disease. There was no difference between the groups in term of systemic medications (Table 2).

Table 3 compares the general ophthalmologic features of individuals with XFS/XFG to those of controls. There was no significant difference in mean IOP, CCT and RNFL thickness between the XFS/XFG and control groups. Since cataract surgery was performed in the control group, the visual acuity was significantly better in this group ($P = 0.03$) than in the XFS/XFG groups. Among the XFS patients, 50% had XFG, most of them in a severe form.

Metabolomics Analysis

After validation of the kit plate based on quality control (QC) samples, 37 (19.7%) metabolites were excluded because of

Table 2. Systemic Medications of Individuals with XFS/XFG Compared to Controls

Systemic Medications	XFS/XFG, $N = 18$	Controls, $N = 16$	*P* Values
Antihypertensive, %	44.44	56.25	0.51
Lipid-lowering medication, %	22.22	31.25	0.57
Antiplatelet therapy/oral anticoagulation, %	16.67	31.25	0.33
Oral diabetes medication, %	16.67	12.5	0.74
Insulin, %	5.56	0	0.33
Corticosteroids, %	0	0	–
Thyroid hormone, %	0	12.5	0.17
Estrogens, %	0	0	–
Vitamin D, %	0	18.75	0.08

Table 3. Ophthalmologic Features and Glaucoma Medications of XFS Patients Compared to Controls

	XFS/XFG, $N = 18$	Controls, $N = 16$	*P* Values
Mean visual acuity, logMAR	0.46	0.05	0.03*
Mean IOP, mm Hg	13.88	14.13	0.8
Mean CCT, µm	544.62	560.00	0.72
Mean RNFL thickness, µm	77.93	84.9	0.12
VF-MD, dB; worse eye	−8.92		
Severity of glaucoma, XFG,%			
No glaucoma	50		
Mild	16.67		
Moderate	11.11		
Severe	22.22		
Glaucoma medication, %			
Beta-blockers	38.88		
Prostaglandin analogue	50		
Alpha-2-agonists	22.22		
Carbonic anhydrase inhibitor	16.67		

* Significant value.

inaccurate measurements. The statistical analysis then was performed on the 151 (80.3%) remaining metabolites (see Supplementary Table S1).

The nonsupervised PCA scatter plot of metabolomics data showed no grouping according to the XFS or control groups, nor any strong outliers in the first principal plan (PC1 versus PC2; Fig. 1A). The OPLS-DA model obtained after the backward procedure comprised only 16 metabolites and provided a good fit for the data ($R^2X = 0.43$, $R^2Y = 0.68$). This model showed good predictive capability ($Q^2cum = 0.51$), with a low risk of over-fitting (permQ2 = −0.48, CV-ANOVA <0.001). A clear discrimination between the XFS and control groups along the predictive component (LV p) was apparent in the scatter plot of the OPLS-DA model (Fig. 1B).

Among the 16 metabolites in the final model, the best discriminant metabolites (with VIP $\geq$ 1 and high absolute Pcorr values) included a subset of six metabolites comprising two medium-chain acyl-carnitines: octanoyl-carnitine (C8) and decanoyl-carnitine (C10), the branched chain amino acids (BCAA) leucine, isoleucine, and valine, and the aromatic amino acid tyrosine (Figs. 2, 3). All these metabolites were at higher concentrations in the XFS group than in the control group. Other metabolites, such as the polyamines spermine and spermidine, four lipids, and the acyl-carnitine octadecenyl-carnitine, were found at lower concentrations in the XFS group than in the control group, but their VIP values were <1. Fold changes, VIPs, and Student's *P* values for all metabolites included in the final OPLS-DA model are shown in Table 4.

Discussion

The plasma metabolomic signature of XFS identified in this study is characterized by increased plasma concentrations of medium chain acyl-carnitines (octanoyl-carnitine C8 and decanoyl-carnitine C10), as well as the increased concentration of four amino acids, namely tyrosine and the three BCAAs; that is, isoleucine, leucine and valine. Indeed, among the 16 metabolites contributing to the OPLS-DA model (Fig. 2), these six metabolites provided the strongest contribution (VIP > 1). The variation of concentration of the 10 other metabolites also contributed to the model, but at a weaker level (0.6 < VIP < 1). Alanine and lysine had increased plasma concentrations, whereas the following metabolites had decreased plasma

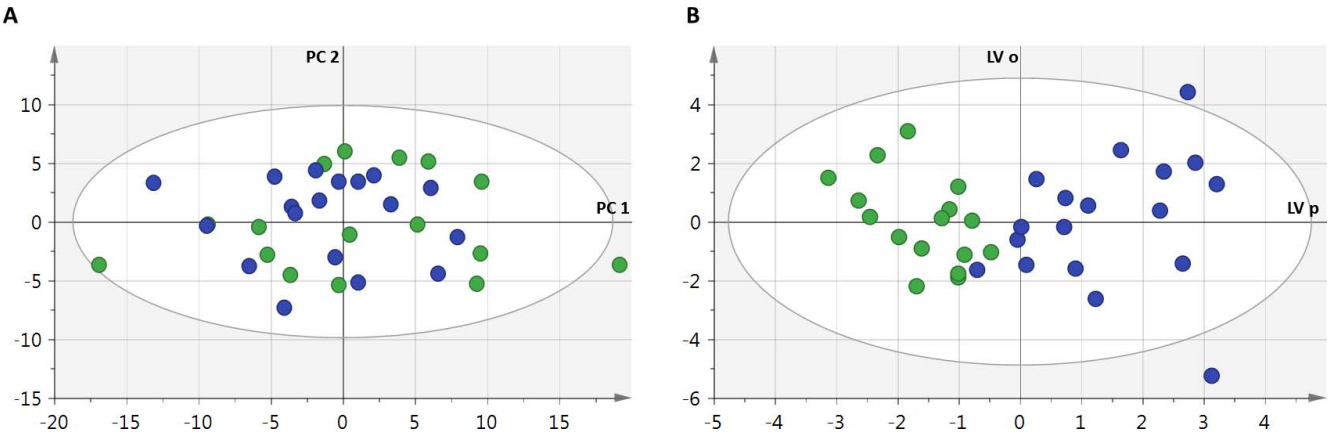

Figure 1. PCA (**A**) and OPLS-DA (**B**) scatter plots obtained from the matrix of metabolites for the 18 XFS patients (*blue circles*) and 16 controls (*green circles*). The PCA scatter plot shows no clearly distinguished trends and the control patient outside the tolerance ellipse is not a strong outlier according to Hotelling's T2 range. The OPLS-DA scatter plot shows a clear distinction between the two groups. PC1,2, principal components 1 and 2; LV p, o, predictive (*p*) and orthogonal (*o*) latent variables, respectively.

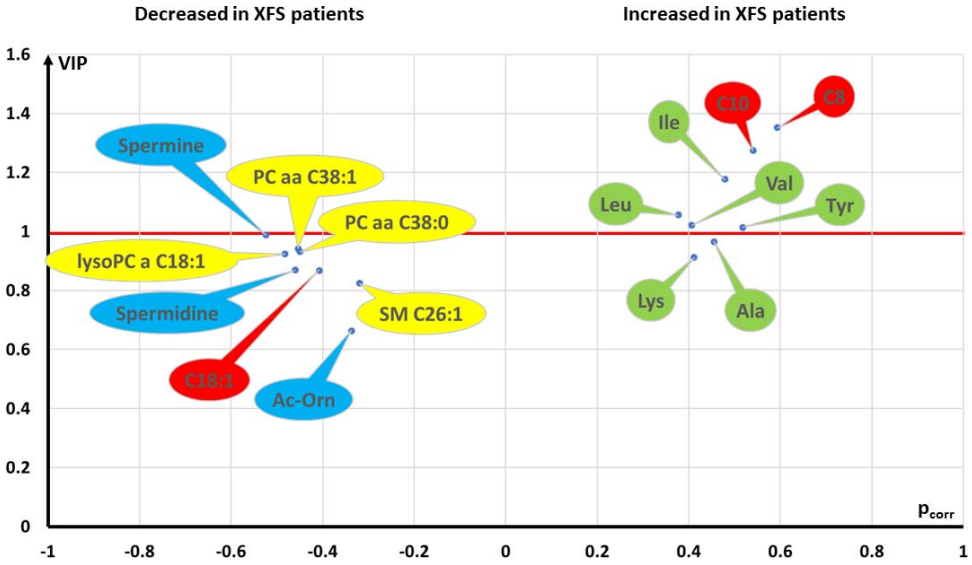

FIGURE 2. Volcano plot (pcorr versus VIP) from the OPLS-DA analysis. All metabolites having VIP > 1 values (above the *red line*) were found in greater concentrations in XFS patients than in controls. This signature was composed by the BCAA: isoleucine (Ile), leucine (Leu), valine (Val), tyrosine (Tyr), and two medium-chain acylcarnitines: octanoylcarnitine (C8) and decanoylcarnitine (C10). Amino acids are represented as *green bubbles*, biogenic amines as *blue bubbles*, acylcarnitines as *red bubbles*, and lipids in *yellow bubbles*. Ala, alanine; Lys, lysine; C18:1, octadecenylcarnitine; Ac-orn, acetyl-ornithine; lysoPC a C18:1, lysophosphatidylcholine C18:1; PC aa C38:0, phosphatidylcholine diacyl C38:0; PC aa 38:1, phosphatidylcholine diacyl C38:1; SM C26:1, sphyngomyeline C26:1. In acyl-carnitines and lipid molecules the length of the acyl chain (two chains for PC) is represented after the "C" while the number of double bonds is indicated after the ":".

concentrations: spermine, phosphatidylcholine diacyl C38:0, phosphatidylcholine diacyl C38:1, lysophosphatidylcholine C18:1, spermidine, octadecenyl-carnitine C18:1, sphingomyelin C26:1, and acetyl-ornithine.

Unexpectedly, this XFS signature overlaps the insulin resistance signature, which also is characterized by increased plasma concentrations of the BCAAs together with other variations of metabolite concentrations.[12,13] However, overlapping of the XFS and insulin resistance signatures is only partial. For instance, compared to the reported insulin resistance signature,[14–16] the XFS signature does not show an increase in the following metabolites, even though they were measured by our kit: hexoses, C3 and C5 short chain acyl-carnitines, phenylalanine, cysteine, glutamate, tryptophan, aspartate, and arginine. In addition, other metabolites, such as glycine, glutamine, methionine, kynurenine, serotonin, and C10 acyl-carnitine, usually found at decreased concentrations in the insulin resistance signature, are not involved in our XFS signature.

Overlapping of the metabolomic signature of XFS with insulin resistance signatures is paradoxical because, to our knowledge, XFS has never been linked either to insulin resistance or to obesity, despite the strong association of XFS with cardiovascular diseases.[5] On the contrary, it appears that diabetes has a lower incidence in XFS individuals compared to the general population or to individuals affected with primary open-angle glaucoma.[17] For instance, a 5.4% prevalence of diabetes mellitus has been reported in XFS individuals versus a 19.2% prevalence in individuals with primary open-angle glaucoma.[18] Another study showed 5% of diabetes mellitus in XFS patients versus 10% in individuals with primary open-angle glaucoma.[19] The reason for this lower frequency of insulin resistance in XFS is unknown. However, the increased concentrations of BCAAs in XFS may have another cause, since a recent meta-analysis including more than 20,000 participants has shown that the level of BCAAs is influenced not only by insulin resistance, but also by the geographic origin, sex, dietary patterns, and genetic background of the patients.[16]

As shown in Tables 1 and 2, the XFS group was similar to the control group regarding sex, BMI, diabetes, dyslipidemia, oral antidiabetic drugs, and insulin treatment. Both groups also were similar for the main systemic medications, but differed for eyedrop therapies given for glaucoma to individuals with XFG. However, to our knowledge, no link has been reported between these eyedrop therapies for glaucoma and the increased plasma concentrations of BCAAs or other compounds identified in the XFS signature. Thus, overlapping of the XFS signature and that of insulin resistance may have a different signification that must be elucidated.

The plasma concentration of tyrosine also was increased in individuals with XFS. Tyrosine is a precursor of dihydroxyphenylalanine (DOPA), dopamine, catecholamines and melanin. Tyrosine also is a precursor of thyroid hormones, but the XFS group was identical to the control group regarding the frequency of thyroid diseases and thyroid medications (Tables 1, 2). In addition, the search in the PubMed database using the keywords "tyrosine" and "glaucoma" or "XFS" failed to show any obvious link. Therefore, hypertyrosinemia may serve as a new biomarker of XFS besides the well-documented XFS-related hyperhomocysteinemia.[5] It is of note that homocysteine was not measured by our kit.

The decreased concentrations in the XFS signature of the polyamines spermine and spermidine, as well as the decreased concentration of their precursor acetyl-ornithine, are interesting findings because spermine and spermidine have an important role in optic nerves.[18] Spermidine and spermine are ubiquitous, naturally occurring polyamines derived from arginine and ornithine metabolism.[20] They also are diet-provided and involved in numerous cellular functions, such as growth, development, nucleic acid and protein syntheses, protein acetylation, and cell signaling. In addition, spermidine

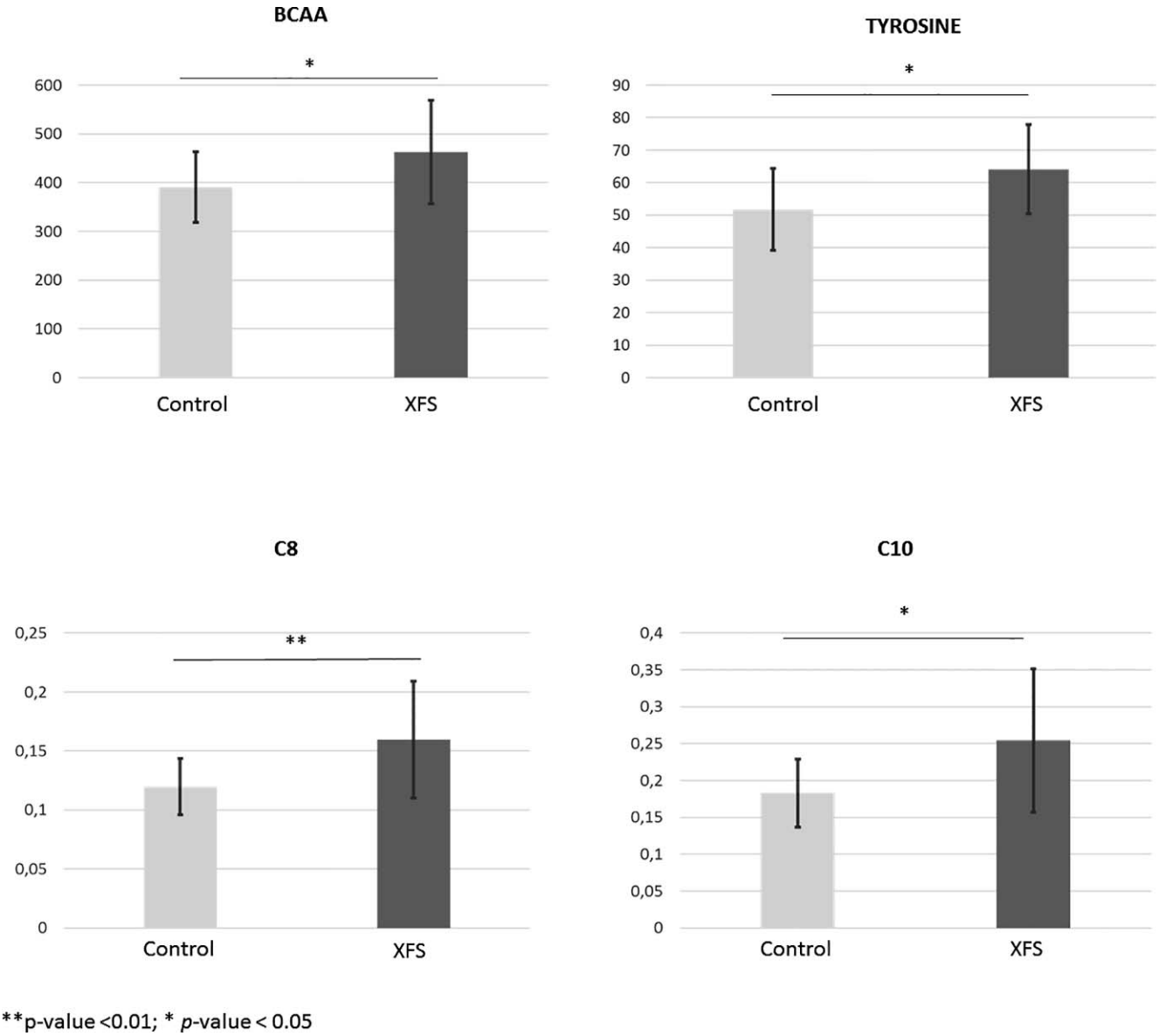

FIGURE 3. Box plot (mean ± SDM) of the BCAA, tyrosine, octanoyl-carnitine (C8), and decanoyl-carnitine (C10) concentration in XFS and control plasmas. All concentrations are in μM/L units and *P* values were obtained using Student's *t*-test.

has antioxidant properties and is a powerful inducer of autophagy that has an important role in longevity.[21] The polyamine concentrations usually decrease with age and their dietary supplementation has been shown to increase longevity in several species, such as in flies, nematodes and mice. The concentration of spermidine in the plasma also is related to longevity in human subjects.[22] The anti-aging effect of spermidine intervenes in the arteries, since spermidine supplementation has been reported to restore the NO-dependent vascular endothelial function in old mice.[20] Age-related XFS being associated with systemic vascular disease, the relative polyamine deficiency observed in the plasma of patients suggests a possible therapeutic target. More specifically, and interestingly in the context of XFG, the spermidine present in the optic nerve,[23] has been shown to have a neuroprotective effect on retinal ganglion cells after optic nerve injury in adult mice.[24] Spermidine also has been reported to prevent retinal ganglion cell neurodegeneration in a mouse model of normal-tension glaucoma.[25] Interestingly, we also have found decreased concentrations of spermine and spermidine in the optic nerve of a transgenic mouse model of dominant optic atrophy carrying a heterozygous mutation in *Opa1*.[26]

In conclusion, we report a significant plasma metabolomic signature in individuals with XFS characterized by decreased concentrations of the neuroprotective spermine and spermidine polyamines, hypertyrosinemia, and a profile partially overlapping the metabolomic signature of insulin resistance. This observation is intriguing because, to our knowledge, no evidence of insulin resistance has been reported in XFS to date. Further investigation will be required to confirm these findings and reveal new insights into the metabolic pathways involved in XFS, hopefully leading to a better understanding of the pathophysiology of the disease.

Table 4. Fold Change, VIP and *P* Values for All Metabolites Retained in the OPLS-DA Model

Metabolites	Fold Changes	VIP	*P* Values
Octanoyl-carnitine, C8	1.33	1.35	0.006
Decanoyl-carnitine, C10	1.39	1.27	0.011
BCAA	1.18		0.029
Isoleucine	1.26	1.18	0.025
Leucine	1.19	1.06	0.074
Valine	1.15	1.02	0.03
Tyrosine	1.24	1.01	0.01
Alanine	1.22	0.97	0.026
Lysine	1.17	0.91	0.045
Spermine	0.48	0.99	0.032
Spermidine	0.89	0.87	0.014
PC aa 38:0	0.79	0.93	0.059
PC aa 38:1	0.68	0.94	0.009
Lyso PC a C18:1	0.82	0.92	0.05
Octadecenyl-carnitine, C18:1	0.81	0.87	0.043
SM C26:1	0.86	0.82	0.1
Acetyl-ornithine	0.72	0.66	0.07

For each metabolite, the fold change was calculated as the ratio between the mean XFS concentration and the mean control concentration**.** lysoPC a C18:1, lysophosphatidylcholine C18:1; PC aa C38:0, phosphatidylcholine diacyl C38:0; PC aa 38:1, phosphatidylcholine diacyl C38:1; SM C26:1, sphyngomyeline C26:1.

Acknowledgments

The authors thank all individuals participating in this study, Kanaya Malkani for critical reading and comments on the manuscript, and Odile Blanchet and the team of the *Centre de Ressources Biologiques* of the University Hospital of Angers for biobank sample processing.

Supported by the Institut National de la Santé et de la Recherche Médicale (INSERM), the Centre National de la Recherche Scientifique (CNRS), University of Angers, University Hospital of Angers, and Région Pays de Loire, and by the following patients' foundations: "Fondation VISIO," "Ouvrir les Yeux," "Union Nationale des Aveugles et Déficients Visuels," "Association contre les Maladies Mitochondriales," "Retina France," "Kjer France," and "Association Point de Mire".

Disclosure: **S. Leruez**, None; **T. Bresson**, None; **J.M. Chao de la Barca**, None; **A. Marill**, None; **G. de Saint Martin**, None; **A. Buisset**, None; **J. Muller**, None; **L. Tessier**, None; **C. Gadras**, None; **C. Verny**, None; **P. Amati-Bonneau**, None; **G. Lenaers**, None; **P. Gohier**, None; **D. Bonneau**, None; **G. Simard**, None; **D. Milea**, None; **V. Procaccio**, None; **P. Reynier**, None

References

1. Lindberg JG. Kliniskaundersokningar over depigmentaring av pupillarranden och genomys barket av iris vid fall av alderstarr samit i normala ogon hos gamla personer (clinical studies of depigmentation of the pupillary margin and transillumination of the iris in case of senile cataract and also in the normal eyes in the aged) [thesis]. Helsinki, Finland: Helsinki University; 1917.
2. Ritch R. Ocular and systemic manifestations of exfoliation syndrome. *J Glaucoma*. 2014;23:S1–S8.
3. Ritch R, Schlotzer-Schrehardt U. Exfoliation syndrome. *Surv Ophthalmol*. 2001;45:265–315.
4. Ahrlich KG, De Moraes CGV, Teng CC, et al. Visual field progression differences between normal-tension and exfoliative high-tension glaucoma. *Invest Ophthalmol Vis Sci*. 2010; 51:1458–1463.
5. Aboobakar IF, Johnson WM, Stamer WD, Hauser MA, Allingham RR. Major review: exfoliation syndrome; advances in disease genetics, molecular biology, and epidemiology. *Exp Eye Res*. 2017;154:88–103.
6. Thorliefsson G, Magnusson KP, Sulem P, et al. Common sequence variants in the LOXL1 gene confer susceptibility to exfoliation glaucoma. *Science*. 2007;317:1397–1400.
7. Aung T, Ozaki M, Mizoguchi T, et al. A common variant mapping to CACNA1A is associated with susceptibility to exfoliation syndrome. *Nat Genet*. 2015;47:387–392.
8. Aung T, Ozaki M, Lee MC, et al. Genetic association study of exfoliation syndrome identifies a protective rare variant at LOXL1 and five new susceptibility loci. *Nat Genet*. 2017;49: 993–1004.
9. McNally S, O'Brien CJ. Metabolomics/proteomics strategies used to identify biomarkers for exfoliation glaucoma. *J Glaucoma*. 2014;23:S51–S54.
10. Hodapp E, Parrish RK II, Anderson DR. *Clinical Decisions in Glaucoma*. St Louis: The CV Mosby Co; 1993:52–61.
11. Eriksson L, Johansson E, Kettaneh-Wold N, Trygg J, Wiksström C, Wold S. *Part I: Basic Principles and Applications PLS. Multi- and Magavariate Data Analysis*. 2nd ed. Umea, Sweden: Umetrics Ed; 2006:85.
12. Shah SH, Bain JR, Muehlbauer MJ, et al. Association of a peripheral blood metabolic profile with coronary artery disease and risk of subsequent cardiovascular events. *Circ Cardiovasc Genet*. 2010;3:207–214.
13. Newgard CB. Interplay between lipids and branched-chain amino acids in development of insulin resistance. *Cell Metab*. 2012;15:606–614.
14. Park S, Sadanala KC, Kim EK. A metabolomic approach to understanding the metabolic link between obesity and diabetes. *Mol Cells*. 2015;38:587–596.
15. Gonzalez-Franquesa A, Burkart AM, Isganaitis E, Patti ME. What have metabolomics approaches taught us about type 2 diabetes? *Curr Diab Rep*. 2016;16:74.
16. Zhao X, Han Q, Liu Y, Sun C, Gang X, Wang G. The relationship between branched-chain amino acid related metabolomic signature and insulin resistance: a systematic review. *J Diabetes Res*. 2016;2016:2794591.
17. Tarkkanen A, Reunanen A, Kivelä T. Frequency of systemic vascular diseases in patients with primary open-angle glaucoma and exfoliation glaucoma. *Acta Ophthalmol*. 2008;86:598–602.
18. Konstas AG, Tsatsos I, Kardasopoulos A, Bufidis T, Maskaleris G. Preoperative features of patients with exfoliation glaucoma and primary open-angle glaucoma. The AHEPA study. *Acta Ophthalmol Scand*. 1998;76:208–212.
19. Tarkkanen A. Pseudoexfoliation of the lens capsule. A clinical study of 418 patients with special reference to glaucoma, cataract, and changes of the vitreous. *Acta Ophthalmol Suppl*. 1962;71:1–98.
20. LaRocca TJ, Henson GD, Thorburn A, Sindler AL, Pierce GL, Seals DR. Translational evidence that impaired autophagy contributes to arterial ageing. *J Physiol*. 2012;590:3305–3316.
21. Rubinsztein DC, Mariño G, Kroemer G. Autophagy and aging. *Cell*. 2011;146:682–695.
22. Pucciarelli S, Moreschini B, Micozzi D, et al. Spermidine and spermine are enriched in whole blood of nona/centenarians. *Rejuvenation Res*. 2012;15:590–595.
23. Ingoglia NA, Sturman JA, Eisner RA. Axonal transport of putrescine, spermidine and spermine in normal and regenerating goldfish optic nerves. *Brain Res*. 1977;130:433–445.
24. Noro T, Namekata K, Kimura A, et al. Spermidine promotes retinal ganglion cell survival and optic nerve regeneration in adult mice following optic nerve injury. *Cell Death Dis*. 2015; 6:e1720.

25. Noro T, Namekata K, Azuchi Y, et al. Spermidine ameliorates neurodegeneration in a mouse model of normal tension glaucoma. *Invest Ophthalmol Vis Sci*. 2015;56:5012–5019.

26. Chao de la Barca JM, Simard G, Sarzi E, et al. Targeted metabolomics reveals early dominant optic atrophy signature in optic nerves of *Opa1*$^{delTTAG/+}$ mice. *Invest Ophthalmol Vis Sci*. 2017;58:812–820.

Investigative Ophthalmology & Visual Science